# The Effect of a Liquid ISSEC on Radiation Damage Parameters in Laser Fusion Reactor First Walls

H.I. Avci and G.L. Kulcinski

April 10, 1977

UWFDM-205

FUSION TECHNOLOGY INSTITUTE

UNIVERSITY OF WISCONSIN

MADISON WISCONSIN

# The Effect of a Liquid ISSEC on Radiation Damage Parameters in Laser Fusion Reactor First Walls

H.I. Avci and G.L. Kulcinski

Fusion Technology Institute
University of Wisconsin
1500 Engineering Drive
Madison, WI 53706

http://fti.neep.wisc.edu

April 10, 1977

UWFDM-205

# The Effect of a Liquid ISSEC on Radiation Damage Parameters in Laser Fusion Reactor First Walls

by

H. I. Avci

G. L. Kulcinski

April 1977

(Revised August 1977)

UWFDM-205

Fusion Technology Program
Nuclear Engineering Department
University of Wisconsin
Madison, Wisconsin 53706

## I. Introduction

The use of a liquid Li ISSEC (Internal Spectral Shifter and Energy Convertor) to protect the first walls of laser fusion reactors has been proposed by scientists at Lawrence Livermore Laboratory.[1] The initial concept involves a 'waterfall' of liquid lithium ranging in thickness from 10-50 cm dropping from the top of a laser fusion reactor to be collected at the bottom of the reaction chamber. The purpose of the waterfall is many fold, and a few of the most obvious reasons are listed below.

- To collect and absorb all photons emitted or reflected from the DT containing fuel pellet.
- To collect all charged particles (unburnt fuel, reaction products and tamper material).
- To moderate the neutrons in order to reduce the damage in the first wall.
- To breed tritium.
- To absorb any shock wave generated in the reaction chamber by the microexplosion.

While there are many questions about the exact mechanism by which this 'waterfall' will be formed, about the rapidity with which the proper geometry can be re-established after the explosion, and about the transmission of the laser light through the vapor generated by the microexplosion, the radiation protection feature of this concept can be estimated at this time.

A great deal of effort has been invested in the study of solid carbon ISSEC's (2,3) with DT and DD fuel (4). More recently solid metallic ISSEC's have been investigated and provide a background against which the present liquid ISSEC's can be assessed.[5] The object of this report is to analyze the effectiveness of a liquid Li ISSEC and briefly compare it to a solid C, V, Nb, Mo and W

ISSEC in terms of displacement damage and gas generation in the first walls. In addition we will propose a liquid Pb (or $Pb_4Li$) ISSEC which may have much more desirable characteristics without sacrificing important parameters such as breeding ratio.

## II. Calculational Procedures

The one-dimensional, homogeneous, cylindrical geometry, model blanket design used in this study is shown in Figure II-1. A variable thickness ISSEC zone was placed between the plasma and the 316 SS first structural wall. An ISSEC density factor (D.F.) of 1.0 was used for neutronic calculations although in practice a density factor of somewhat less than 1.0 would be appropriate (this would result in a thicker ISSEC region). However, the neutron "optical" thickness would be the same in both cases. The solid materials previously studied for an ISSEC were[(5)] carbon, molybdenum, niobium, vanadium and tungsten. These solid ISSEC's are then compared to liquid Li and Pb ISSEC's.

The first wall material used in all cases was 316 SS with 1 cm thickness at a D. F. of 0.5. The first wall is followed by a 60 cm thick breeding zone composed of 95% natural lithium and 5% 316 SS for structural material. Behind the breeding zone is a 30 cm thick reflector zone with a composition of 95% C and 5% 316 SS. Both the breeding zone and the reflector zone have a D. F. of 1.0 although in reality in the reflector zone a D. F. of less than 1.0 would be more appropriate to take into account the coolant passages. To simulate the final shield albedos of 0.05, 0.10, 0.20, 0.25 were used for neutron groups 1 through 5 (9 to 14.9 MeV), respectively. An albedo of 0.3 was used for neutrons of lower energy.

The nuclear performance of this type of reactor design was studied by solving the discrete ordinates form of the neutron transport equation for

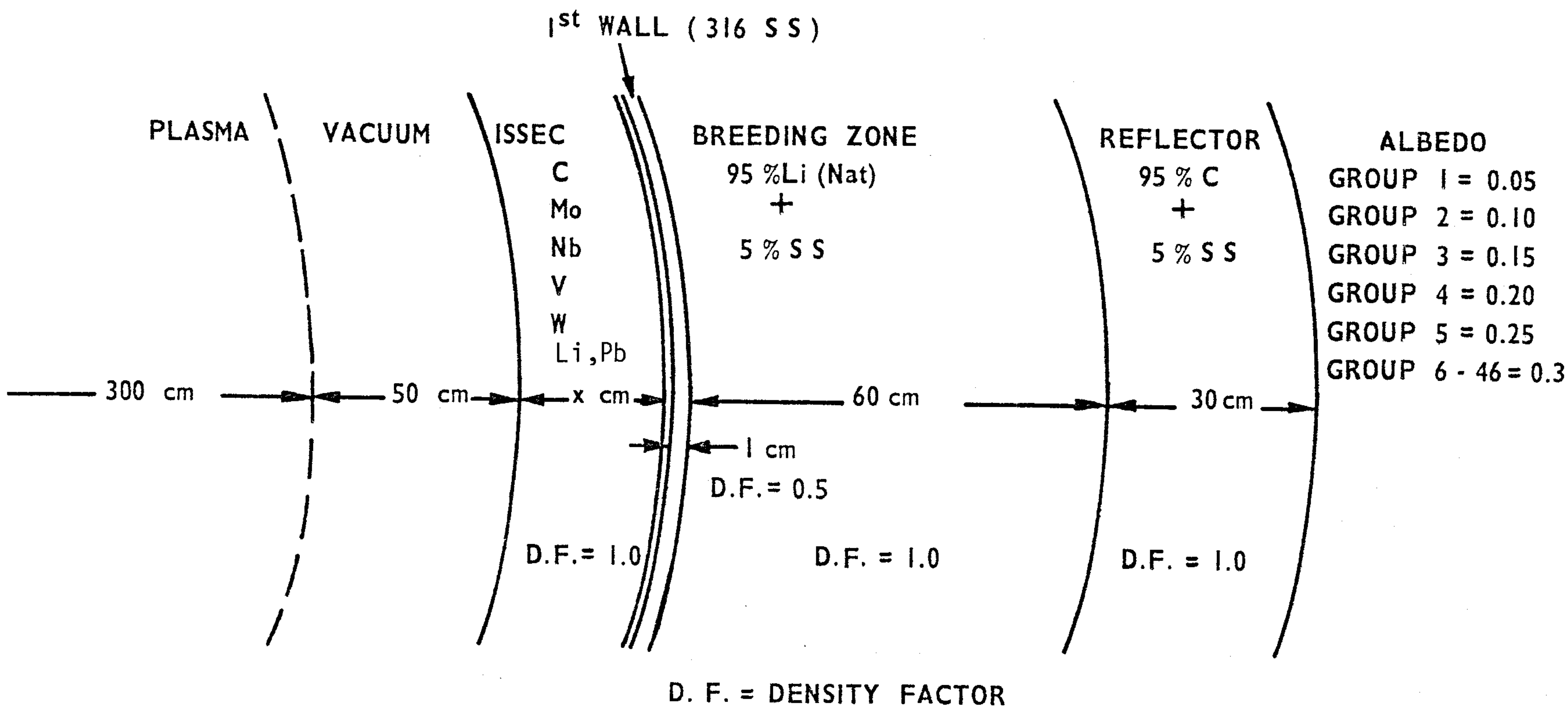


1 - DIMENSIONAL CYLINDRICAL BLANKET MODEL USED IN THIS STUDY

Figure II-1

a cylinder using the ANISN[6] program with a $S_4$-$P_3$ approximation. It has been shown elsewhere[7] that this approximation is adequate to predict integral parameters such as tritium breeding and gas production rates to within approximately 2% of a higher order calculation like the $S_{16}$-$P_5$. A uniform cylindrical source was used consistently with our previous study for tokamaks[5]. Obviously the neutron source from the pellet is different but it was felt that, for the sake of consistency, we would retain the uniform source and corrections for source geometry can be made in the future.

The neutron and gamma production cross sections were obtained as a coupled set of 100 neutron groups and 21 gamma groups produced for EPR calculations.[8] This data set was generated with the AMPX modular code system[9] from nuclear data in ENDF/B-IV. The only exception is Nb where evaluation of the cross sections is based on ENDF/B-III data. (Previous calculations in references 2 to 4 were all based on ENDF/B-III data).

Due to the costs and computer memory limitations, the 100 neutron group cross sections were collapsed to 46 groups keeping the same fine group structure above 2 MeV as in the original set. The 46 group neutron and 21 group gamma interaction cross sections' group structures used in these calculations, are given in Appendix A.

Neutron kerma factors were generated using the MACK program[10] based on data in ENDF/B-III. The gamma kerma factors were calculated using the MUG[11] code and ENDF/B-III data.

The displacement cross sections were calculated from a computer code developed by Doran[12]. The values used in these calculations are given in references 3 and 4.

All results are normalized to 1 $MW/m^2$ neutronic wall loading, i.e., 1 MW of neutron energy passing through the first wall (or inner ISSEC surface) per $m^2$ of area.

## III. Results

Information obtained in this study falls into 3 general categories.

A.) Damage parameters in the first 316 SS wall

B.) Overall breeding ratio

C.) Heat deposition profiles

Let us examine each one separately.

A.) Damage Parameters

1.) Displacement Damage

The effect of the various ISSEC thicknesses on the reduction in displacement damage is listed in table III-1 and plotted in figure III-1. Without ISSEC protection the first wall will suffer ~10 dpa per year at 1 $MW/m^2$ (100% PF). Inserting 20 cm of material in front of the wall reduces this damage by a factor of ~2 for Li and Pb up to a maximum of ~30 for tungsten. The effectiveness of the various ISSECs increases with atomic weight mainly because of the increased inelastic scattering cross sections which reduce the overall energy spectrum. The exception to this is Pb which has a very high (n,2n) cross section at 14 MeV (~2 barns) and a very low absorption cross section. This results in considerable neutron multiplication and even though the energy of the neutrons from the (n,2n) reaction are lower than the incident 14 MeV neutrons, they are usually in the MeV range where the displacement cross section is still very high. Hence, the damage from the increased neutron flux partially offsets the reduction in damage due to a softening of the neutron spectrum.

It was found that extending the ISSEC thickness to 40 cm dropped the dpa rate by a factor of 4 from the unprotected case and a 1 meter waterfall would reduce the damage in the 316 SS to ~5% of that in the bare wall. This

Table III-1

Summary of Radiation Damage in 316 SS First Wall Behind Various ISSEC's

| ISSEC Material | dpa/yr (1 MW/$m^2$) | appm He/yr (1 MW/$m^2$) | appm H/yr (1 MW/$m^2$) |
|---|---|---|---|
| None | 10.1 | 218 | 470 |
| | 20 cm | | |
| Li | 5.4 | 82 | 210 |
| C | 2.5 | 27 | 85 |
| V | 1.5 | 10 | 23 |
| Nb | 1.3 | 5 | 12 |
| Mo | 0.9 | 4 | 10 |
| W | 0.45 | 2 | 5 |
| Pb | 4.8 | 14 | 37 |
| | 40 cm | | |
| Li | 2.8 | 32 | 96 |
| Pb | 2.6 | 1.8 | 5.4 |
| | 100 cm | | |
| Li | 0.5 | 2.0 | 10.5 |
| Pb | 0.4 | 0.004 | 0.4 |

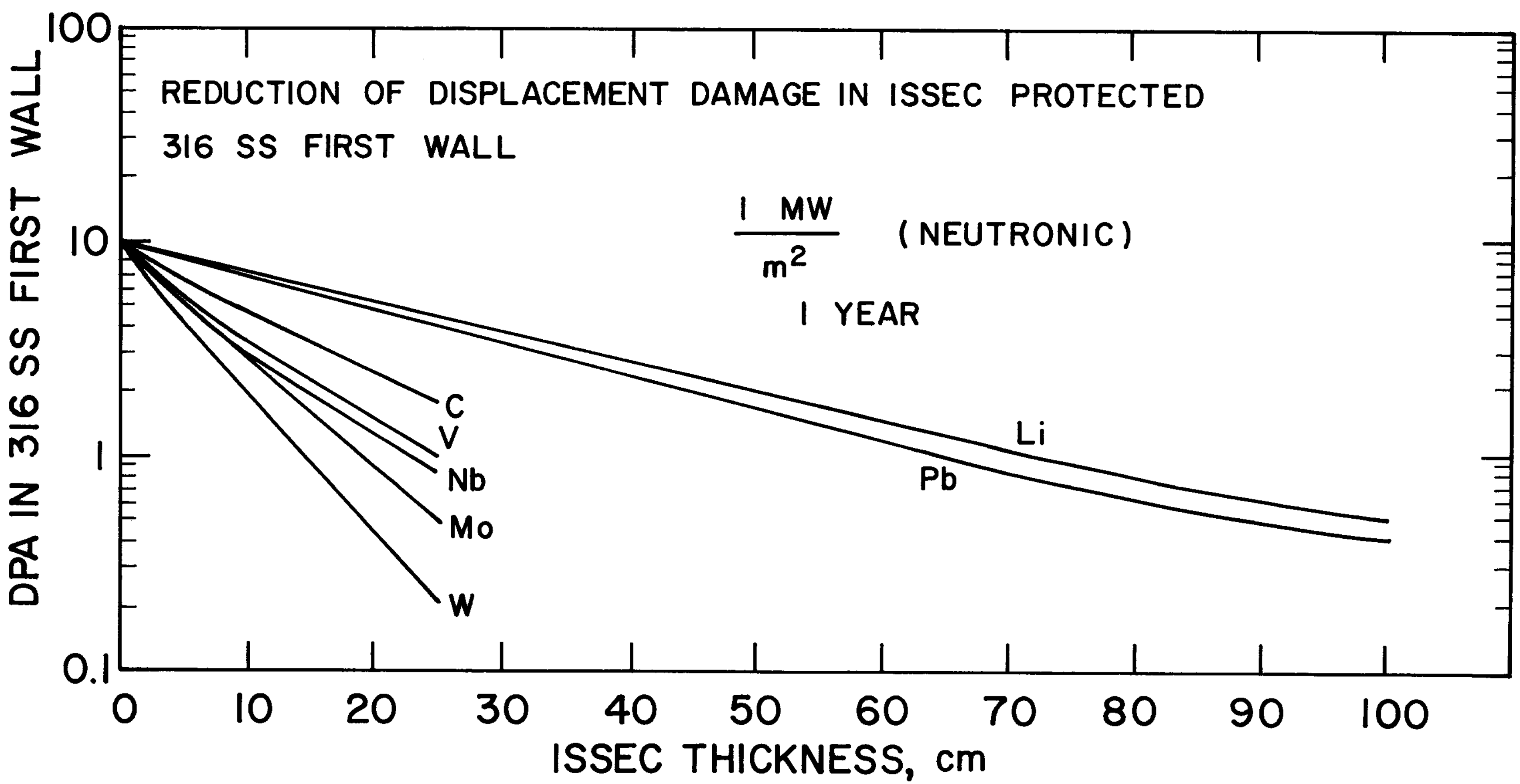
REDUCTION OF DISPLACEMENT DAMAGE IN ISSEC PROTECTED
316 SS FIRST WALL
1 MW/m2 (NEUTRONIC)
1 YEAR
DPA IN 316 SS FIRST WALL
100
10
1
0.1
C
V
Nb
Mo
W
Li
Pb
0
10
20
30
40
50
60
70
80
90
100
ISSEC THICKNESS, cm

Figure III-1

rate of reduction corresponds to roughly a factor of 2 reduction for every 20 cm of liquid Li or Pb.

2.) Gas Production

The reduction in the helium and hydrogen production rates with varying thicknesses of ISSEC are also given in table III-1 and plotted for helium in Figure III-2.

We only plot the results for He here as the results for the hydrogen isotopes are qualitatively the same. There are two main differences between the helium reaction rates and displacement rates. First, the relative effectiveness of all the ISSECs is greater; that is, the amount of reduction per unit ISSEC thickness is greater. Twenty cm of ISSEC can reduce the helium production rates from a factor of 2.7 for Li to a factor of 16 for Pb and a factor of 100 for W. Increasing the liquid ISSEC thickness to 40 cm gives an overall reduction of ~7 for Li and 120 for Pb. If the liquid ISSECs are increased to 1 m in thickness, the Li will reduce the helium production rates by a factor of ~110 over the unprotected case and Pb will reduce it by about a factor of 55,000!

The second point of notice in the helium production rates is that unlike the case of displacement damage where Pb and Li were essentially the same, now lead is much more effective in reducing the overall helium production rate than is Li. This is easily understood by noting that the (n,$\alpha$) threshold for most of the isotopes in steel is in the neighborhood of 3-5 MeV. Hence, the extra neutron flux from the (n,2n) reactions probably does not contribute to the helium production like it did to the displacement rates and the softening of the spectrum is now very effective.

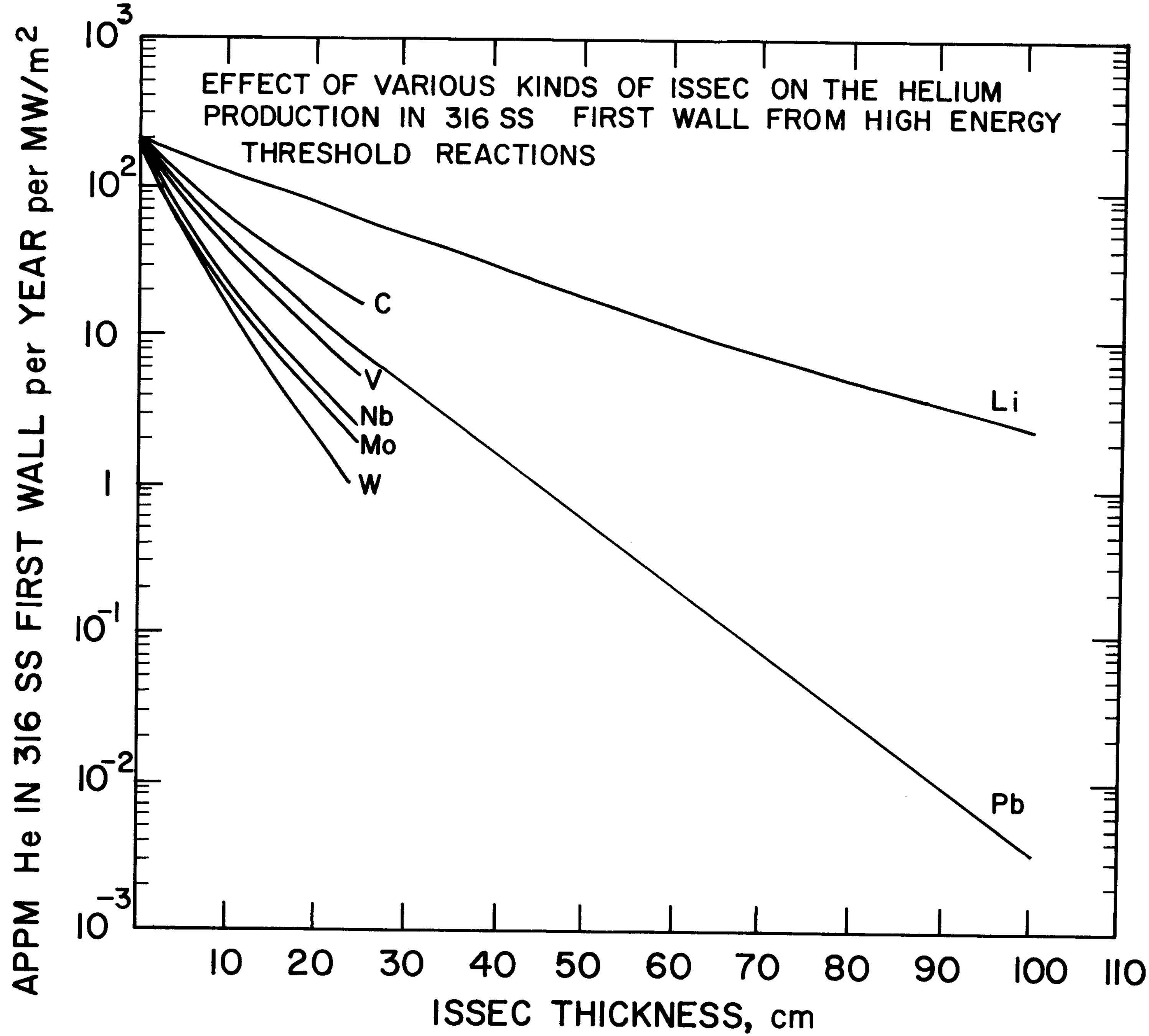
EFFECT OF VARIOUS KINDS OF ISSEC ON THE HELIUM PRODUCTION IN 316 SS FIRST WALL FROM HIGH ENERGY THRESHOLD REACTIONS
APPM He IN 316 SS FIRST WALL per YEAR per MW/m2
10^3
10^2
10
1
10^-1
10^-2
10^-3
10
20
30
40
50
60
70
80
90
100
110
ISSEC THICKNESS, cm
C
V
Nb
Mo
W
Li
Pb

Figure III-2

B.) Breeding Ratio

The detailed information on the overall breeding ratio is given in table III-2 and plotted in figure III-3. We only include the detailed information on the liquid ISSECs here and the reader is referred to a previous paper for the data on the solid ISSECs.[5]

A general inspection of figure III-3 reveals that whereas the solid C, V, Nb, Mo and W ISSECs all reduce the breeding ratio in the lithium behind the first wall to values of less than 1 in 5 to 20 cm, the use of a liquid Pb ISSEC actually increases the breeding to ~1.7 at 20 cm thickness. The breeding ratio only drops to below 1.0 only after ~94 cm of Pb ISSEC. The reason for this is again related to the high (n,2n) cross section and the low parasitic absorption in Pb. Since the threshold for the $Li^7$ $(n,n\alpha)T$ reaction is ~2.5 MeV, the production of neutrons below that energy does not help the breeding ratio at all. The Pb softens the neutron spectrum such that behind a thickness of ~40 cm there are not enough neutrons above 2.5 MeV to produce a significant amount of tritium by the Li-7 reaction and eventually parasitic absorption in the Pb and structure cause the breeding by Li-6 to be reduced below one.

The increase in the total breeding ratio for the Li ISSEC is as expected and perhaps the only surprising point is that there still is significant tritium production from Li-6 in the blanket behind a 1 meter Li region.

C.) Heat Extraction

The amount of neutron and gamma heating in the ISSEC, first wall, and blanket region is given in table III-3 and the total energy per neutron is plotted in figure III-4. The fraction of energy absorbed in the ISSEC is plotted in figure III-5. Let us analyze the details of table III-3 first.

Table III-2

Summary of Tritium Breeding Data in Liquid

Li and Pb ISSEC Systems

| | | Tritium atom per incident neutron* | | | | | | |
|---|---|---|---|---|---|---|---|---|
| | | Breeding in 'Waterfall' | | | Breeding in Blanket | | | Overall B. R. |
| ISSEC | Thickness-cm | $T_6^I$ | $T_7^I$ | $T_{tot}^I$ | $T_6^B$ | $T_7^B$ | $T_{tot}^B$ | $T_{tot}$ |
| Li | 0 | -- | -- | -- | 0.892 | 0.608 | 1.50 | 1.50 |
| | 23 | 0.305 | 0.527 | 0.832 | 0.641 | 0.266 | 0.907 | 1.74 |
| | 46 | 0.538 | 0.747 | 1.285 | 0.449 | 0.117 | 0.566 | 1.85 |
| | 115 | 0.904 | 0.902 | 1.806 | 0.131 | 0.009 | 0.140 | 1.95 |
| Pb | 0 | -- | -- | -- | 0.892 | 0.608 | 1.50 | 1.50 |
| | 22 | -- | -- | - | 1.632 | 0.047 | 1.679 | 1.68 |
| | 45 | -- | -- | -- | 1.595 | 0.005 | 1.600 | 1.60 |
| | 112 | -- | -- | -- | 0.771 | $4 \times 10^{-6}$ | 0.771 | 0.77 |

I = ISSEC

B = Blanket

* $T_6$ and $T_7$ denote breeding from $Li^6$ and $Li^7$ isotopes in natural lithium, respectively.

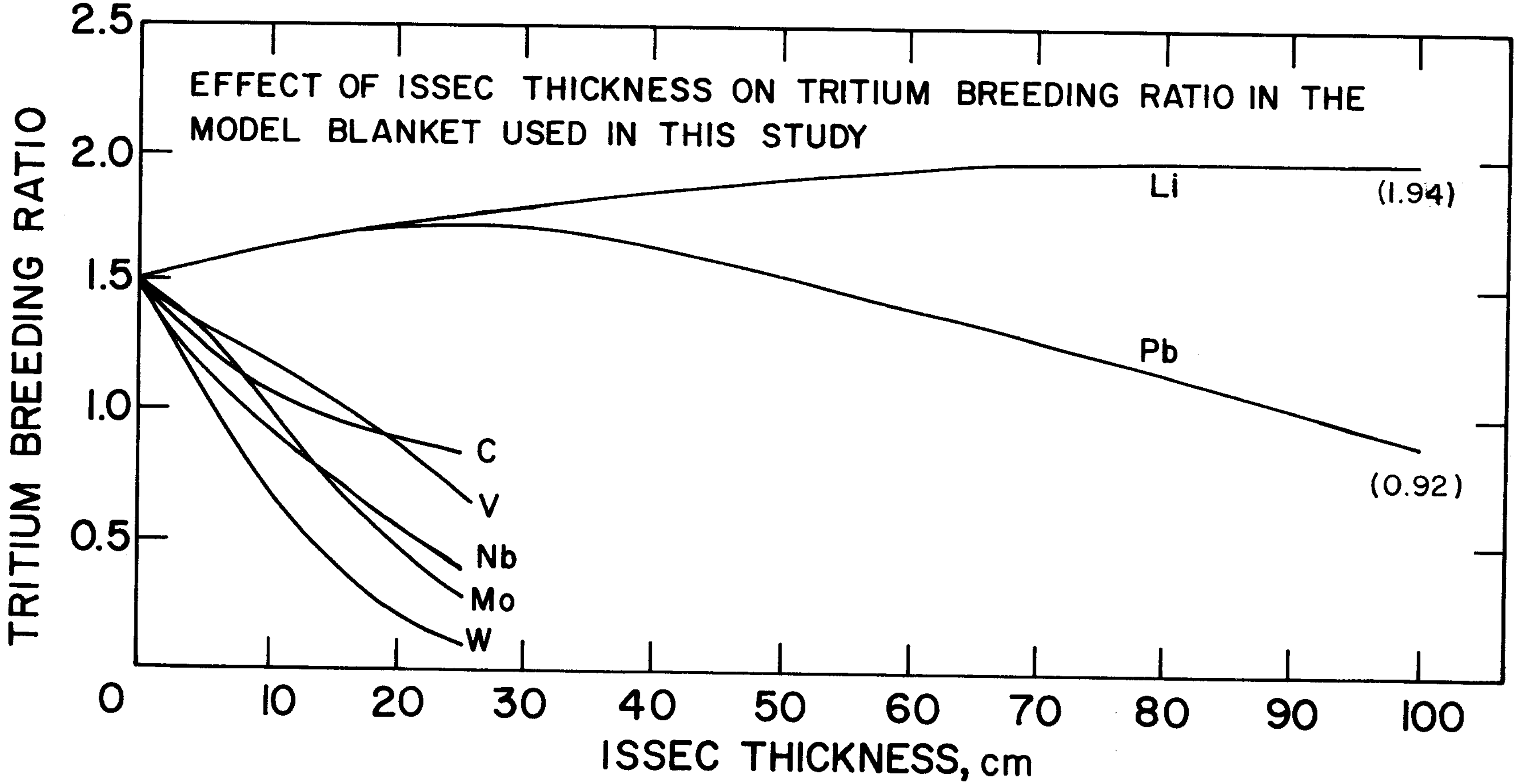
EFFECT OF ISSEC THICKNESS ON TRITIUM BREEDING RATIO IN THE MODEL BLANKET USED IN THIS STUDY
TRITIUM BREEDING RATIO
2.5
2.0
1.5
1.0
0.5
0
10
20
30
40
50
60
70
80
90
100
ISSEC THICKNESS, cm
Li
(1.94)
Pb
(0.92)
C
V
Nb
Mo
W

Figure III-3

Table III-3

Summary of Heat Extraction Data in a Liquid ISSEC Protected Laser Fusion Reactor

| ISSEC | Thickness cm | Source | ISSEC | MeV/n 316 SS First Wall | Breeding Zone | Reflector | Total ISSEC + Blanket | Total Energy Production[(a)] |
|---|---|---|---|---|---|---|---|---|
| Li | 0 | n | - | 0.25 | 12.0 | 0.4 | 12.65 | |
| | | γ | - | 0.39 | 2.3 | 0.76 | 3.45 | |
| | | | | | | | | 19.6 |
| | 23 | n | 7.34 | 0.11 | 6.55 | 0.19 | 14.20 | |
| | | γ | 0.30 | 0.16 | 1.11 | 0.40 | 1.98 | |
| | | | | | | | | 19.7 |
| | 46 | n | 10.97 | 0.04 | 3.74 | 0.08 | 14.83 | |
| | | γ | 0.43 | 0.10 | 0.58 | 0.22 | 1.33 | |
| | | | | | | | | 19.7 |
| | 115 | n | 14.63 | 0.004 | 0.77 | 0.006 | 15.41 | |
| | | γ | 0.63 | 0.023 | 0.096 | 0.037 | 0.79 | |
| | | | | | | | | 19.7 |
| Pb | 0 | n | - | 0.25 | 12.0 | 0.4 | 12.65 | |
| | | γ | - | 0.39 | 2.3 | 0.76 | 3.45 | |
| | | | | | | | | 19.6 |
| | 22 | n | 0.43 | 0.034 | 9.35 | 0.08 | 9.89 | |
| | | γ | 5.93 | 0.051 | 0.54 | 0.43 | 6.95 | |
| | | | | | | | | 20.4 |
| | 45 | n | 0.79 | 0.011 | 8.26 | 0.03 | 9.09 | |
| | | γ | 7.84 | 0.030 | 0.25 | 0.29 | 8.41 | |
| | | | | | | | | 21.0 |
| | 112 | n | 1.31 | 0.001 | 3.76 | 0.003 | 5.07 | |
| | | γ | 15.34 | 0.018 | 0.12 | 0.064 | 15.54 | |
| | | | | | | | | 24.13 |

(a) Includes 3.52 MeV alpha particle energy.

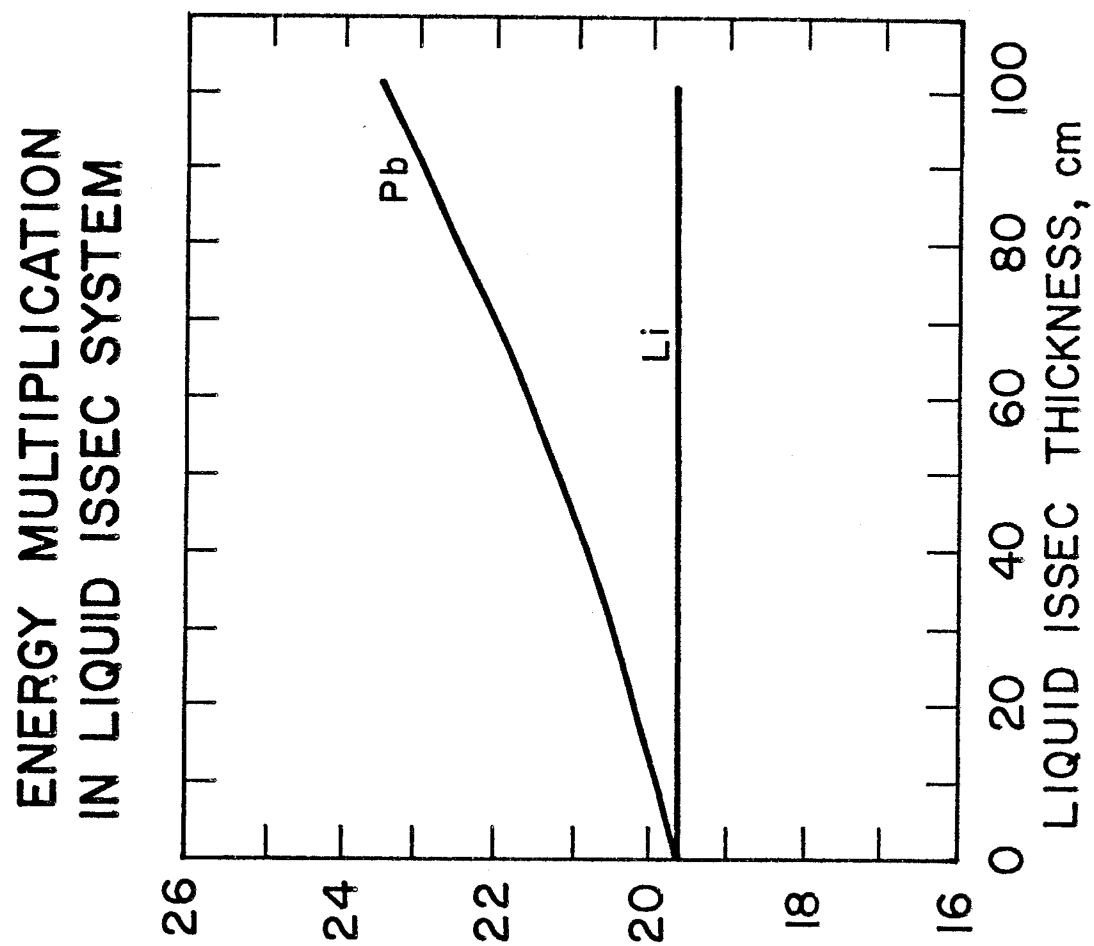
ENERGY MULTIPLICATION
IN LIQUID ISSEC SYSTEM
ENERGY per NEUTRON, (Mev/n)
LIQUID ISSEC THICKNESS, cm
Pb
Li
26
24
22
20
18
16
0
20
40
60
80
100

Figure III-4

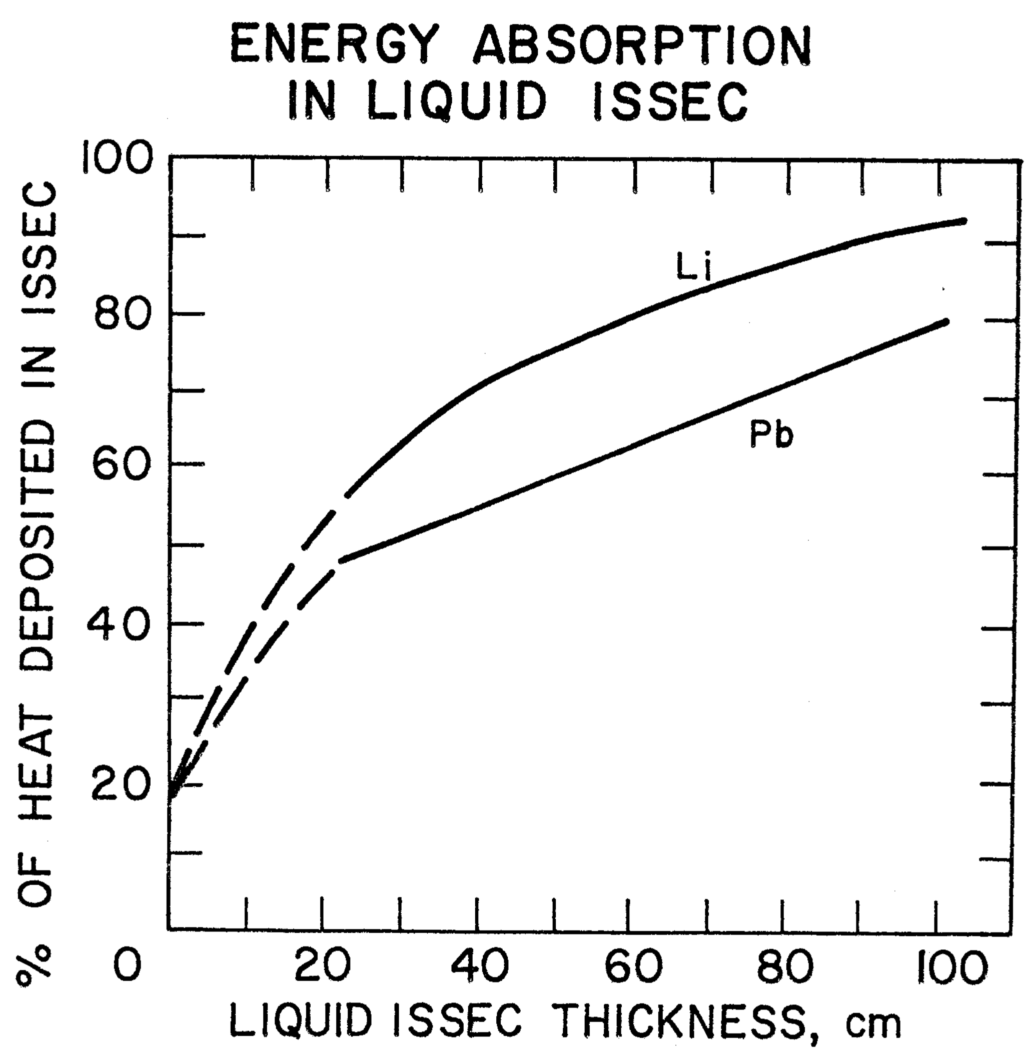
ENERGY ABSORPTION
IN LIQUID ISSEC
% OF HEAT DEPOSITED IN ISSEC
100
80
60
40
20
0
20
40
60
80
100
LIQUID ISSEC THICKNESS, cm
Li
Pb

Figure III-5

As expected, the amount of energy extracted from the ISSEC increases as the thickness increases. The liquid ISSECs effectively relieve the neutron and gamma ray heating in the first wall and reduce the heating to insignificant levels. The lead is more effective than the Li in this regard.

The major difference between the Pb and Li ISSECs is their response to neutrons and gammas. There is little nuclear heating in the Pb because of the low parasitic absorption cross section, but high $\gamma$ heating because of the high absorption coefficient for photons. The situation is opposite in the Li where the nuclear heating is large because of the exothermic Li-6 $(n,\alpha)$ reaction, but the gamma heating is correspondingly small because of the weak absorption for photons.

Another major difference between the Li and Pb ISSECs is that there is still considerable nuclear heating in the Li behind the first wall after a 100 cm thick Pb ISSEC. This is, of course, due to the tritium breeding from Li-6.

The energy per neutron values (including the 3.52 MeV alpha particle) are also listed in table III-3 and shown in figure IV-4. The value for the blanket in figure II-1 without any ISSEC protection is 19.6 MeV/n and it stays surprisingly constant as the thickness of the Li ISSEC is increased. On the other hand, there is considerable energy multiplication from the Pb system, presumably due to the extra neutrons and the fact that most of the tritium now comes from the exothermic Li-6 reactions instead of the endothermic Li-7 reaction. The energy per neutron increases from 19.6 MeV/n with no Pb

ISSEC to 20.3 with a 20 cm Pb zone, 20.8 with 40 cm and 23.5 with a 1 meter thick zone. This latter number represents a 20% increase in the energy production over a non-protected blanket.

The fraction of heat absorbed in the liquid ISSEC (including the charged particles) is plotted in figure III-5 and it shows that for thickness of 20-30 cm, the ISSEC zone will generate > 50% of the heat. The fraction of heat collected in the Li ISSEC is always higher than the Pb system even though the absolute values are about the same. Ninety percent of the heat in a liquid Li system is deposited in 90 cm of liquid ISSEC and only 8% of the total heat is left for the blanket behind a 100 cm liquid Li zone.

Proportionately less energy is absorbed in the Pb ISSEC because of the breeding behind the first wall. Almost 20% of the total heat generated in that system remains to be collected in the blanket even after a 100 cm thick ISSEC zone is used. Methods to alleviate this problem will be discussed later.

## IV. Discussion

There are five features of this work which should be emphasized as far as first wall protection and blanket design are concerned.

1) The relatively small effect liquid Li and Pb ISSECs have on displacement damage.
2) The large effect Pb has on reducing helium production.
3) The very favorable breeding from both liquid Li and Pb systems.
4) The optimum thickness to get maximum wall life within working constraints of an operating system.
5) The high energy multiplication.

Aside from protecting the first walls of a laser fusion reactor against high fluxes of photons and charged particles (which could be done by a relatively thin stream of liquid) it is important to see what beneficial effect the concept can have on extending the useful first wall lifetime.

For an illustrative example we will consider 316 SS at three different temperatures; 600°C, 500°C, and 300°C. The criteria for failure is different in each of these temperature ranges. Helium embrittlement is the limiting feature of 600°C, void swelling is the problem at 500°C, and crack propagation and helium gas bubble swelling is critical at 300°C. While the exact dpa and helium limits are not known for these regimes, we have made a conservative estimate on the basis of our past experience. The projections are shown in Table IV-1. Assuming that we desire to have a "permanent" first wall for 30 years of operation at a nominal wall loading of 5 $MW/m^2$ and a plant factor of 70%, we can use the information in table IV-1 to estimate the required ISSEC thickness. The necessary ISSEC thickness is given in table IV-2.

Table IV-1

Estimate of Damage Limitations in 316 SS Irradiated in a Fusion Neutron Spectrum

| | Design Limit | |
|---|---|---|
| Temperature °C | dpa | appm He |
| 300 | 200* | 4000 |
| 500 | 150* | 500* |
| 600 | 100 | 10* |

* Limiting Parameter

Table IV-2

Summary of Liquid Metal ISSEC Thickness Required to Extend 316 SS First Wall Life to Reactor Life[a]

| Temperature °C | Required ISSEC Thickness-cm | | | |
|---|---|---|---|---|
| | Li | | Pb | |
| | dpa | He | dpa | He |
| 300 | 52 | 47 | 47 | 12 |
| 500 | 58 | ~85 | 52 | 30 |
| 600 | 74 | ~200 | 67 | 67 |

(a) 5 $MW/m^2$ at 70% P.F. for 30 years. (1060 dpa, 22,900 appm He accumulated for an unprotected wall).

The required ISSEC thickness to reduce the dpa level to the value desired at end of life (Table IV-1) falls in the general range of 45 to 75 cm for both Li and Pb. The requirements from the helium generation levels are generally more severe for Li and it is found that the ISSEC thickness must be much greater than 1 meter and probably on the order of 2 meters for 600°C operation. The Li thickness required for protection against excessive helium generation is ~85 cm at 500°C and it drops to ~47 cm at 300°C. The constraints are much more relaxed for Pb since it is more effective at reducing helium production than displacement damage. The results in table IV-2 show that as little as 12 cm of Pb will suffice for 316 SS operating at 300°C and 67 cm is required to allow very high temperature operation.

A summary of what the approximate optimum ISSEC thickness might be is given in table IV-3. The thickness of ISSEC required was chosen and all the other parameters are associated with that parameter. It can be seen that at a first wall temperature of 300°C either 52 cm of Li or 47 cm of Pb will reduce the total dpa level to 200 in 30 years. However, the Pb ISSEC yields more energy (7%) and reduces the helium production to a level 20 times less than the equivalent thickness of Li. On the other hand, the BR is 20% higher in the Li protected first wall concept.

The required ISSEC thickness is 85 cm for Li and 52 cm for Pb at 500°C. These values are determined by dpa considerations for Pb and helium considerations for Li. The Pb ISSEC again produces more energy than the Li ISSEC (8%) and the helium production rate is a factor of 9.3 lower. The Li ISSEC has a much higher breeding ratio (~27%) although both systems have quite adequate breeding.

Finally, at 600°C it is seen that over 2 meters of Li is required to reduce the helium production rate such that no more than 10 appm accumulate

Table IV-3

Summary of Necessary Liquid ISSEC Thicknesses Required to Extend Useful Lifetime of 316 SS to 30 Years at 70% P.F. and 5 $MW/m^2$ Wall Loading

System Parameters

| Temperature °C | Thickness cm | dpa/yr | Appm He/yr | B.R. | MeV/n | % Energy in ISSEC |
|---|---|---|---|---|---|---|
| | | | Lithium | | | |
| 300 | 52 | 6.67* | 63 | 1.9 | 19.7 | 77 |
| 500 | 85 | 2.4 | 16.7* | 1.9 | 19.7 | 89 |
| 600 | ~200 | ~0.02 | ~ 0.33* | ~2 | 19.7 | ~100 |
| | | | Lead | | | |
| 300 | 47 | 6.67* | 2.8 | 1.58 | 21.0 | 59 |
| 500 | 52 | 5.0* | 1.8 | 1.50 | 21.3 | 61 |
| 600 | 67 | 3.3* | 0.34* | 1.34 | 22.2 | 67 |

*Design Limit

over 30 years. The Pb ISSEC can conform to the design limits ( by coincidence it is both the dpa and appm He in this case) in table IV-1 with only a 67 cm zone. Another advantage of the Pb is that the energy per neutron is now 13% higher and an adequate BR can be maintained (1.34). One advantage of the 2 meter Li ISSEC is that essentially all the heat is collected in the ISSEC and there is no need for the blanket to either generate tritium or run at a high temperature!

The last example shows that there is a thickness above which it probably makes no sense to run the first wall hot because there is very little heat to collect. For example, it is entirely conceivable that one could collect the last 10% of the energy at 300°C and not suffer very greatly on overall efficiency. Such a limit is at 90 cm for the Li system and ~120 cm for the Pb system.

The concept of 'cold' first walls and blankets (~ The Li could run at ~250°C) has a great attractiveness because it would significantly reduce the complexity of the reactor design and perhaps even the tritium leakage.

One final point is worth noting about the ratio of helium production to displacement damage. The characteristic values for a fast fission reactor (EBR-II), a LWR (HFIR), a bare wall, and various thicknesses of Li and Pb ISSEC's are given in table IV-4.

It can be seen that whereas the helium to dpa ratio is very high in an unprotected first wall, it is very low in a fast fission reactor. This unfavorable ratio has been responsible for the lack of interest in using these facilities for test beds. On the other hand, placing approximately 60-70 cm of lead in front of the first wall reduces that ratio to a value commensurate with the fast reactor. If the materials scientists knew that the first

Table IV-4

Ratio of Helium Production to Displacement Damage in ISSEC System

| ISSEC | Thickness-cm | Appm He/dpa in 316 SS |
|---|---|---|
| Li | 20 | 15 |
| | 40 | 11 |
| | 100 | 4 |
| Pb | 20 | 3 |
| | 40 | 0.7 |
| | 100 | 0.01 |
| Fusion | 0 | 20 |
| EBR-II | - | 0.1 |
| HFIR | - | ~100 |

walls would experience that ratio of gas to displacement damage in fusion reactors, they could take advantage of the information generated in the fast reactor program and thereby save a lot of time and money for future design analysis.

## V.) Conclusions

It has been shown that both Li and Pb liquid ISSEC's are rather ineffective at reducing displacement damage in the first walls of a laser fusion reactor until the thickness approaches 50 cm or more. Lead is much more effective at reducing helium gas effects than Li and in fact, 70 cm of Pb could reduce the total helium production in 30 years to levels comparable to or less than already generated in EBR-II irradiated material. Lead has an added advantage that it increases the energy production per neutron by ~10% (~ 30-40 $MW_e$ in a 1000 $MW_t$ plant) and breeding ratios of greater than 1.0 are attainable for thicknesses up to 95 cm. It appears that 30 year first wall lifetimes can be achieved at a Pb ISSEC thickness of 47 to 67 cm if the first wall is run between 300 to 600°C respectively. The corresponding figures for Li are 52 to 200 cm for 300 to 600°C respectively.

## VI. Suggestions for Future Work

After assessing the effectiveness of liquid lead and lithium separately, we have the following suggestions for an improved system.

1) A liquid Pb-Li alloy should be investigated as the ISSEC.
2) The thickness of a Pb-Li alloy required to satisfy the dpa, gas production and breeding ratio requirements should be determined.
3) A possible reactor design which requires no tritium breeding behind the first wall and allows the blanket to run "cold" should be investigated.
4) Neutron spectra from high $\rho R$ pellets should be included in the designs to see if thinner "waterfalls" can be used for the same reductions in critical damage parameters.

The Pb-Li phase diagram is shown in Figure VI-1 and it reveals the existence of an eutectic at 235°C. The composition of this eutectic is $Pb_4Li$. Work is now in progress on calculating the same dpa, gas production, B.R., etc. parameters as a function of ISSEC thickness that were calculated for this paper. It is expected that the simultaneous slowing down and capture of the neutrons before they impinge on any solid member will result in even further reduced damage rates. However, the most significant effects of using a Pb-Li alloy will probably be that one can maintain a B.R. of greater than one in the ISSEC alone and that most of the heat can be collected in the ISSEC as opposed to the pure lead system. This would remove the need for tritium breeding (hence energy generation) behind the first wall and hence the problem of high temperatures. The walls can be made of almost any material compatible with cooling water and low partial pressures of Pb and Li.

A crude schematic of a reactor concept based on these ideas is shown in Figure VI-2. The key feature of this design is that the liquid $Pb_4Li$ is completely removed from the reactor to accomplish heat extraction and tritium removal leaving the first wall and blanket to be an independent and separate structure.

Acknowledgement

This research was supported by a grant from the Energy Research and Development Administration, Division of Laser Fusion Energy, under contract #RP-237.3.

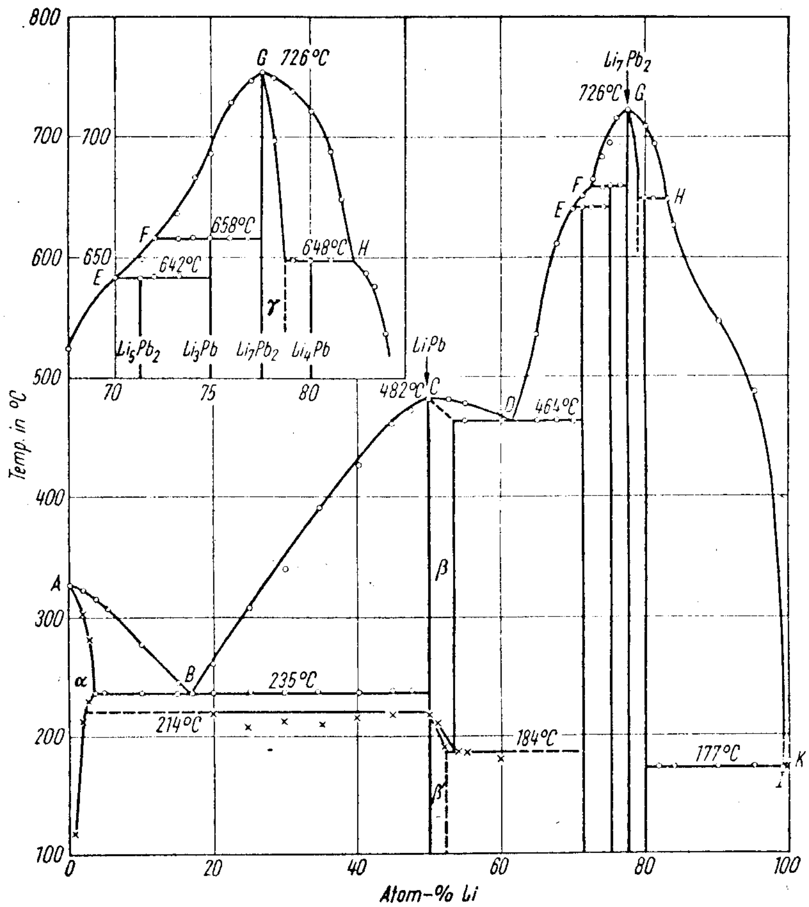


Pb–Li-Zustandsdiagramm.

Figure VI-1

Phase Diagram for Pb-Li[14]

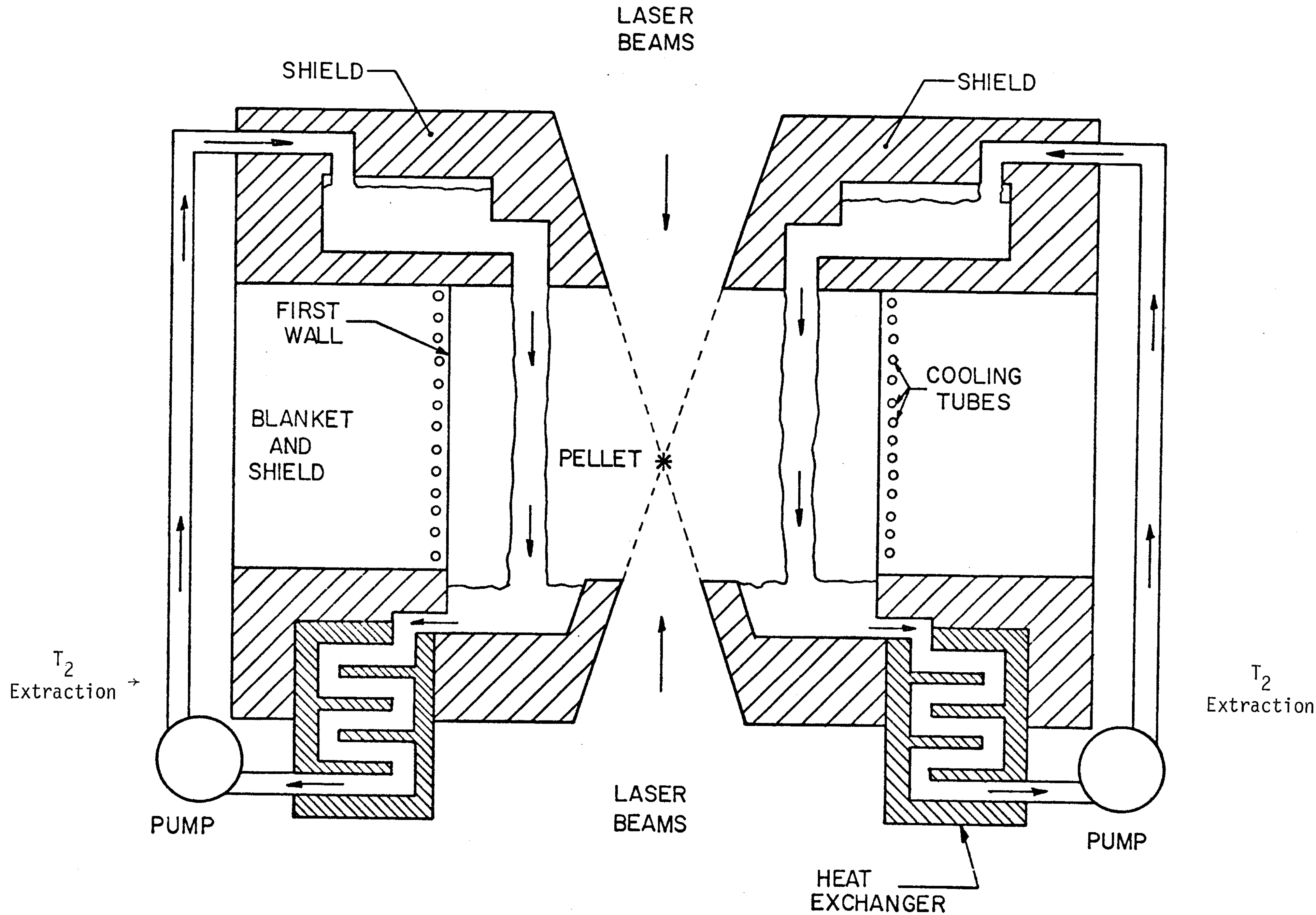


Figure VI-2
Schematic of Possible Li-Pb Alloy Waterfall Concept

## References


1. J. Maniscalco, to be published.

2. R. W. Conn, G. L. Kulcinski, H. Avci, and M. El-Maghrabi, Nucl. Tech. 26, 125, 1975.

3. G. L. Kulcinski, R. W. Conn, H. I. Avci, D. K. Sze, "Production of CTR Metallic First Walls by Neutron Spectral Shifting", Report UWFDM-127, Nuclear Engr. Dept., University of Wisconsin, June 1975. Also Trans. Am. Nucl. Soc. 21, 50 (1975).

4. H. I. Avci and G. L. Kulcinski, "The Response of ISSEC Protected First Walls to DT and DD Plasma Nuetrons," Proc. Int. Confer. on Rad. Eff. and Tritium Tech. for Fusion Reactors at Gatlinburg, Tennessee, October 1-3, 1975. Also Report UWFDM-135, Nucl. Engr. Dept., Univ. of Wis., Madison, Wisconsin, October 1975.

5. H. I. Avci, Y. Gohar, T. Y. Sung, G. L. Kulcinski and C. W. Maynard, UWFDM-202, April 1977.

6. W. W. Engle, Jr., "A Users Manual for ANISN," K-1693, Oak Ridge Gaseous Diffusion Plant.

7. D. J. Dudziak, "Fusion Reactor Nuclear Analysis-Methods and Applications," 8th Symp. on Fusion Technology, Noordijkerhout, The Netherlands, June 1974.

8. D. M. Plaster, R. T. Santoro, and W. E. Ford III, "Coupled 100 Group Neutron and 21 Group Gamma Ray Cross Sections for EPR Calculations," ORNL-TM-4872, April 1975.

9. N. M. Greene, et al., "AMPX: A Modular Code System for Generating Coupled Multi-group Neutron-Gamma Libraries From ENDF/B", ORNL-TM-3706, Oak Ridge National Lab.

10. M. Abdou, C. W. Maynard, and R. W. Wright, "MACK: A Program to Calculate Neutron Energy Release Parameters (fluence to Kerma Factors) and Multi-group Neutron Reaction Cross Sections From Nuclear Data in ENDF Format," ORNL-TM-3994.

11. J. R. Knight and F. R. Mynatt, "MUG: A Program for Generating Multi-group Photon Cross Sections," CTC-17 (January 1970).

12. D. G. Doran, Nucl. Sci. Engr. 52, 398, 1973. See also Nucl. Sci. Engr. 49, 130, 1972.

13. G. L. Kulcinski, D. G. Doran, and M. A. Abdou, "Comparison of Displacement and Gas Production Rates in Current Fission and Future Fusion Reactors," ASTM STP 570, 1975, pp. 329-351.

14. Gmelins Handbuch Der AnorganischenChemie Blei - Teil C3, System #47, pub. 1970 - p. 979.

Appendix A



Neutron and Gamma Energy Multigroup Structures Used in This Study

TABLE A.1

Neutron 46 Multigroup Structure in eV

| Group | Group Limits E(Top) | Group Limits E(Low) | E(Mid-Point) |
|---|---|---|---|
| 1 | 1.4918 (+7) | 1.3499 (+7) | 1.4208 (+7) |
| 2 | 1.3499 (+7) | 1.2214 (+7) | 1.2856 (+7) |
| 3 | 1.2214 (+7) | 1.1052 (+7) | 1.1633 (+7) |
| 4 | 1.1052 (+7) | 1.0000 (+7) | 1.0526 (+7) |
| 5 | 1.0000 (+7) | 9.0484 (+6) | 9.5242 (+6) |
| 6 | 9.0484 (+6) | 8.1873 (+6) | 8.6178 (+6) |
| 7 | 8.1873 (+6) | 7.4082 (+6) | 7.7977 (+6) |
| 8 | 7.4082 (+6) | 6.7032 (+6) | 7.0557 (+6) |
| 9 | 6.7032 (+6) | 6.0653 (+6) | 6.3843 (+6) |
| 10 | 6.0653 (+6) | 5.4881 (+6) | 5.7767 (+6) |
| 11 | 5.4881 (+6) | 4.9659 (+6) | 5.2270 (+6) |
| 12 | 4.9659 (+6) | 4.4933 (+6) | 4.7296 (+6) |
| 13 | 4.4933 (+6) | 4.0657 (+6) | 4.2795 (+6) |
| 14 | 4.0657 (+6) | 3.6788 (+6) | 3.8722 (+6) |
| 15 | 3.6788 (+6) | 3.3287 (+6) | 3.5038 (+6) |
| 16 | 3.3287 (+6) | 3.0119 (+6) | 3.1703 (+6) |
| 17 | 3.0119 (+6) | 2.7253 (+6) | 2.8686 (+6) |
| 18 | 2.7253 (+6) | 2.4660 (+6) | 2.5956 (+6) |
| 19 | 2.4660 (+6) | 1.8268 (+6) | 2.1464 (+6) |
| 20 | 1.8268 (+6) | 1.3534 (+6) | 1.5901 (+6) |
| 21 | 1.3534 (+6) | 1.0026 (+6) | 1.1700 (+6) |
| 22 | 1.0026 (+6) | 7.4274 (+5) | 3.726 (+5) |
| 23 | 7.4274 (+5) | 5.5023 (+5) | 6.4648 (+5) |
| 24 | 5.5023 (+5) | 4.0762 (+5) | 4.7892 (+5) |
| 25 | 4.0762 (+5) | 3.0197 (+5) | 3.5480 (+5) |
| 26 | 3.0197 (+5) | 2.2371 (+5) | 2.6284 (+5) |
| 27 | 2.2371 (+5) | 1.6573 (+5) | 1.9472 (+5) |
| 28 | 1.6573 (+5) | 1.2277 (+5) | 1.4425 (+5) |
| 29 | 1.2277 (+5) | 6.7379 (+4) | 9.508 (+4) |
| 30 | 6.7379 (+4) | 3.1828 (+4) | 4.9604 (+4) |

Table A.1 (cont.)

| Group | Group Limits E(Top) | E(Low) | E(Mid-Point) |
|---|---|---|---|
| 31 | 3.1828 (+4) | 1.5034 (+4) | 2.3431 (+4) |
| 32 | 1.5034 (+4) | 7.1017 (+3) | 1.1068 (+4) |
| 33 | 7.1017 (+3) | 3.3546 (+3) | 5.2281 (+3) |
| 34 | 3.3546 (+3) | 1.5846 (+3) | 2.4696 (+3) |
| 35 | 1.5846 (+3) | 7.4852 (+2) | 1.1666 (+3) |
| 36 | 7.4852 (+2) | 3.5358 (+2) | 5.5105 (+2) |
| 37 | 3.5358 (+2) | 1.6702 (+2) | 2.6030 (+2) |
| 38 | 1.6702 (+2) | 7.8893 (+1) | 1.2296 (+2) |
| 39 | 7.8893 (+1) | 3.7267 (+1) | 5.8080 (+1) |
| 40 | 3.7267 (+1) | 1.7603 (+1) | 2.7435 (+1) |
| 41 | 1.7603 (+1) | 8.3152 (+0) | 1.2959 (+1) |
| 42 | 8.3153 (+0) | 3.9279 (+0) | 6.1216 (+0) |
| 43 | 3.9279 (+0) | 1.8554 (+0) | 2.8917 (+0) |
| 44 | 1.8554 (+0) | 8.7643 (-1) | 1.3659 (+0) |
| 45 | 8.7643 (-1) | 4.1399 (-1) | 6.4521 (-1) |
| 46 | 4.1399 (-1) | 2.2000 (-2) | 2.1800 (-1) |

TABLE A.2

Gamma 21 Multigroup Structure in MeV

| Group | Group Boundaries E(Top) | E(Low) | E(mid-Point) |
|---|---|---|---|
| 1 | 1.2E01 | 1.4E01 | 1.30E01 |
| 2 | 1.0E01 | 1.2E01 | 1.10E01 |
| 3 | 8.0E00 | 1.0E01 | 9.00E00 |
| 4 | 7.5E00 | 8.0E00 | 7.75E00 |
| 5 | 7.0E00 | 7.5E00 | 7.25E00 |
| 6 | 6.5E00 | 7.0E00 | 6.75 E00 |
| 7 | 6.0E00 | 6.5E00 | 6.25E00 |
| 8 | 5.5E00 | 6.0E00 | 5.75E00 |
| 9 | 5.0E00 | 5.5E00 | 5.25E00 |
| 10 | 4.5E00 | 5.0E00 | 4.75E00 |
| 11 | 4.0E00 | 4.5E00 | 6.25E00 |
| 12 | 3.5E00 | 4.0E00 | 3.75E00 |
| 13 | 3.0E00 | 3.5E00 | 3.25E00 |
| 14 | 2.5E00 | 3.0E00 | 2.75E00 |
| 15 | 2.0E00 | 2.5E00 | 2.25E00 |
| 16 | 1.5E00 | 2.0E00 | 1.75E00 |
| 17 | 1.0E00 | 1.5E00 | 1.25E00 |
| 18 | 4.0E-01 | 1.0E00 | 7.00E-1 |
| 19 | 2.0E-01 | 4.0E-01 | 3.00E-1 |
| 20 | 1.0E-01 | 2.0E-01 | 1.50E-1 |
| 21 | 1.0E-02 | 1.0E-01 | 5.00E-2 |